

Theory of surface sum frequency generation spectroscopy

Jesús A. Maytorena

Facultad de Ciencias, Universidad Autónoma del Estado de Morelos, Avenida Universidad 1001, 62210 Cuernavaca, Morelos

Bernardo S. Mendoza

Centro de Investigaciones en Optica, Apartado Postal 1-948, 37000 León, Guanajuato

W. Luis Mochán

Laboratorio de Cuernavaca, Instituto de Física, Universidad Nacional Autónoma de México, Apartado Postal 48-3, 62251 Cuernavaca, Morelos

(Received 6 March 1997)

We develop simple models for the calculation of optical sum and difference frequency generation spectra at the surface of isotropic centrosymmetric conductors and insulators. One of them consists of a semi-infinite free electron gas with a continuously varying electronic density profile. The other consists of a continuous distribution of polarizable entities that respond nonlinearly to the gradient of the field. We solve the Euler equations for the former ignoring the pressure term. Assuming the response of each polarizable entity to be described by that of a harmonic oscillator, we solve the second model incorporating multipolar contributions to the macroscopic surface and bulk polarization. For both models we obtain analytical expressions that produce the nonlinear bulk and surface susceptibilities in terms of the bulk dielectric response of the system. We found an electric-field-induced second-order magnetic moment whose contribution to the susceptibilities is as large as that of the electric dipolar and quadrupolar moment. This contribution is absent in the particular case of second harmonic generation and has not been discussed previously in the literature. By choosing the appropriate dielectric functions we obtain the approximate nonlinear response and frequency conversion efficiency for different systems. [S0163-1829(98)02803-3]

I. INTRODUCTION

The electric-dipolar quadratic susceptibility is a third rank tensor, and therefore it must be null within the bulk of any centrosymmetric system. As second-order nonlinear processes, dipolar sum and difference frequency generation (SFG and DFG) from centrosymmetric systems are only allowed at an interface where inversion symmetry is broken. For this reason, a large portion of the light with frequency $\omega_3 = \omega_1 \pm \omega_2$ reflected from an interface illuminated with two monochromatic beams at ω_1 and ω_2 is surface originated, making SFG/DFG sensitive optical surface probes for this class of systems. Besides being nondestructive and non-invasive, SFG/DFG has the added advantage of accessing surfaces such as buried interfaces, out of ultrahigh-vacuum conditions and within arbitrary transparent ambients.

The use of SFG as a surface probe was introduced in 1987.¹ Most SFG experiments have been directed towards the observation of adsorbed overlayers whose vibrational modes may be probed by tuning one of the fundamental frequencies in the infrared.²⁻¹⁰ In this case, the frequency resolution is comparable to that of IR linear reflectance spectroscopy, but the relative sensitivity to the surface vs the bulk is four to five orders of magnitude larger,¹¹ as the surface contribution to the linear reflectance is of the order of the seldedge's width divided by the wavelength. SFG has also been used to explore surfaces such as electrolyte-metal interfaces.¹¹ Although most of the attention has been centered on the adsorbed molecules, the nonlinear response of the substrate itself is also of interest.¹² The surface electronic

structure has also been explored by SFG in buried interfaces such as SiO₂-Si,¹³ where its versatility was employed to elucidate the nature of a resonance detected with second-harmonic generation (SHG). Although SFG and SHG share many features as surface probes, SFG is more versatile, as the propagation and polarization directions of each of the fundamental beams, as well as their frequencies, may be independently varied.

In spite of the experimental work done for ten years on surface SFG, a theoretical understanding of it is barely emerging. It is only very recently that the angular dependence of SFG on isotropic surfaces has been investigated in terms of the independent components of the bulk and surface nonlinear susceptibilities and their symmetry-originated constraints.¹⁴ Only some of these components have been calculated for jellium models.¹⁴ Some crystallinity effects have also been incorporated, but only for the bulk of an anisotropic electron gas model.¹⁵ The purpose of the present paper is the development of approximate models that permit the calculation of all the components of the surface and bulk second-order response tensors of arbitrary centrosymmetric semi-infinite homogeneous conductors and insulators. These models constitute a natural extension of previous work¹⁶ on second-harmonic generation.

As a first step we develop a simple model conductor that consists of a semi-infinite isotropic electron gas with an equilibrium density profile that interpolates smoothly between its vacuum and bulk asymptotic values. We set up the Euler hydrodynamic equation for this system ignoring the pressure term but including a dissipative term and the nonlinearities

due to the convective time derivative and the Lorentz force. We solve it to obtain the nonlinear induced current at the surface and at the bulk of the conductor, and from the result we identify the nonlinear susceptibility. Our analytical results are similar to those of Ref. 14, but we obtain two independent bulk response functions; one of them canceled fortuitously in Ref. 14 but no longer null when dissipation is present. Furthermore, we obtained a new definite expression for the response normal to the surface, although it has the flaws expected due to the lack of spatial dispersion in our model.¹⁷

A second model, applicable to dielectric surfaces, consists of a homogeneous semi-infinite distribution of polarizable entities that respond harmonically to the perturbing field and field gradients. This distribution is characterized by the dipoles' number density, which interpolates continuously across the surface from zero in vacuum to its constant value at the bulk, and we assume the microscopic response functions of all dipoles to be the same. The origin of the nonlinearity in this case is the spatial variation of the field across each dipole. This variation gives a small contribution of order a/λ in the bulk, where a is the size of each polarizable entity and λ is the optical wavelength. However, the normal component of the electric field has a very rapid variation at the surface, in a scale much smaller than λ , thus yielding a sizable surface nonlinear macroscopic polarization. We calculate the electric dipolar and quadrupolar, as well as a magnetic dipolar contribution to this polarization. Remarkably, the latter does not contribute to the polarization in the degenerate case of second harmonic generation, and therefore its importance for the nonlinear response in the nondegenerate case had not been recognized previously. Finally, we obtain analytical expressions which are exact within our model for the surface and bulk parameters in terms of the linear dielectric functions $\epsilon(\omega_1)$, $\epsilon(\omega_2)$, and $\epsilon(\omega_3)$.

We employ the results of Ref. 14 to derive explicit formulas for the the SFG/DFG radiated efficiency in terms of all the non-null susceptibility components and the dielectric response of the system. We use these expressions to calculate the efficiency of a model solid made up of harmonic polarizable entities. Furthermore, by substituting the appropriate dielectric response we can approximate the SFG/DFG spectra of arbitrary systems. We illustrate this procedure by calculating the efficiency of a Si crystal and we compare the results to experiment.

The paper is organized as follows: In Sec. II we present our models for conductors (II A) and dielectrics (II B), and we solve them to obtain the surface and bulk susceptibility tensors. Using a suitable parametrization of the susceptibilities we also obtain the radiation efficiency for SFG. In Sec. III, we evaluate the formulae obtained in Sec. II for a harmonic solid and for Si. In Sec. IV we present the conclusions of the present work and finally in the Appendix we present some results required for the calculation of the SFG efficiency.

II. THEORY

In this section we obtain analytical expressions for the surface and bulk nonlinear susceptibilities of simple models

for conductor and for dielectric materials, and for the SFG/DFG radiation efficiency.

A. Jellium model of conductors

Consider a simple metal modeled by a classical charged fluid made of electrons of charge $-e$ and mass m , whose equation of motion is given by Euler equation ignoring the pressure term,

$$mn\left(\frac{\partial}{\partial t} + \frac{1}{\tau}\right)\vec{u} + mn(\vec{u} \cdot \nabla)\vec{u} = -en\vec{E} - \frac{e}{c}n\vec{u} \times \vec{B}, \quad (1)$$

where $n = n(\vec{r}, t)$ is the electronic density at point \vec{r} and time t , \vec{u} is the velocity field, and \vec{E} and \vec{B} are the electric and magnetic field, respectively. We expand the time-dependent quantities as a superposition of monochromatic waves with frequencies ω_1 , ω_2 , $2\omega_1$, $2\omega_2$, and $\omega_1 \pm \omega_2$; we have

$$\begin{aligned} f(\vec{r}, t) = & f_0(\vec{r}) + f(\vec{r}, \omega_1)e^{-i\omega_1 t} + f(\vec{r}, \omega_2)e^{-i\omega_2 t} \\ & + f(\vec{r}, 2\omega_1)e^{-i2\omega_1 t} + f(\vec{r}, 2\omega_2)e^{-i2\omega_2 t} \\ & + f(\vec{r}, \omega_1 + \omega_2)e^{-i(\omega_1 + \omega_2)t} \\ & + f(\vec{r}, \omega_1 - \omega_2)e^{-i(\omega_1 - \omega_2)t} + \dots + \text{c.c.}, \quad (2) \end{aligned}$$

where f stands for either n , \vec{u} , \vec{E} , or \vec{B} , c.c. stands for the complex conjugate of the previous terms, and we remark that in equilibrium only the density $n_0(\vec{r})$, is different from zero. An alternative definition of the amplitudes $f(\vec{r}, \omega)$ is through $f(\vec{r}, t) = \dots + \text{Re}f(\vec{r}, \omega)e^{-i\omega t} + \dots$. Both definitions lead to different results for nonlinear problems. Although the difference is trivial, i.e., some extra powers of 2 appear in the response functions, it has to be kept in mind.

Using expansion (2) in Eq. (1), we generate a series of equations for the f variables that oscillate at the same frequency. In this way, the solution for the velocity field at the fundamental frequencies ω_i , with $i=1,2$, is given by

$$\vec{u}(\omega_i) \equiv \vec{u}_i = -i \frac{e/m}{\Omega_i} \vec{E}_i, \quad (3)$$

to linear order in the field, where $\Omega_i = \omega_i + i/\tau$, and $\vec{E}_i \equiv \vec{E}(\omega_i)$. We define the polarization $\vec{J} = \partial \vec{P} / \partial t$, so that

$$\vec{P}_i \equiv \vec{P}(\omega_i) = -\frac{\vec{J}_i}{i\omega_i}, \quad (4)$$

where $\vec{J}_i \equiv \vec{J}(\omega_i)$ is the induced current,

$$\vec{J}_i = -en_0\vec{u}_i, \quad (5)$$

from which we get the linear polarization

$$\vec{P}_i = -\frac{e^2/m}{\omega_i\Omega_i}n_0\vec{E}_i. \quad (6)$$

Now, from the continuity equation and Eq. (3), we obtain the first-order induced density as

$$n(\omega_i) \equiv n_i = \frac{e/m}{\omega_i \Omega_i} \nabla \cdot (n_0 \vec{E}_i). \quad (7)$$

Now we concentrate on the equation for $\vec{u}_3 \equiv \vec{u}(\omega_3)$, where $\omega_3 = \omega_1 + \omega_2$ corresponds to the SF response. From Eq. (1) we get to second-order in the field

$$\begin{aligned} & -i\Omega_3 \vec{u}_3 + (\vec{u}_1 \cdot \nabla) \vec{u}_2 + (\vec{u}_2 \cdot \nabla) \vec{u}_1 \\ & = -\frac{e}{m} \vec{E}_3 + \frac{ie}{m} \left[\frac{1}{\omega_2} \vec{u}_1 \times (\nabla \times \vec{E}_2) + \frac{1}{\omega_1} \vec{u}_2 \times (\nabla \times \vec{E}_1) \right]. \end{aligned} \quad (8)$$

Substituting the linear velocity (3), we can solve Eq. (8) for \vec{u}_3 in terms of the electric field at the fundamental frequencies. In this case the induced current \vec{J}_3 is given by

$$\vec{J}_3 = -en_0 \vec{u}_3 - en_1 \vec{u}_2 - en_2 \vec{u}_1, \quad (9)$$

from which we finally obtain the SF (quadratic) polarization as

$$\begin{aligned} \vec{P}_3 = & -\frac{e^2/m}{\omega_3 \Omega_3} n_0 \vec{E}_3 - \frac{e^3/m^2}{\omega_3 \Omega_3} n_0 \left[\frac{1}{\omega_1 \Omega_1} (\vec{E}_1 \cdot \nabla) \vec{E}_2 \right. \\ & + \left. \frac{1}{\omega_2 \Omega_2} (\vec{E}_2 \cdot \nabla) \vec{E}_1 \right] + \frac{e^3/m^2}{\omega_1 \omega_2 \Omega_1 \Omega_2} \left[\frac{\omega_1}{\omega_3} \nabla \cdot (n_0 \vec{E}_2 \vec{E}_1) \right. \\ & + \left. \frac{\omega_2}{\omega_3} \nabla \cdot (n_0 \vec{E}_1 \vec{E}_2) \right] + \frac{e^3/m^2}{\omega_3 \Omega_3} \frac{n_0}{\omega_1 \omega_2 \Omega_1 \Omega_2} \{ \omega_1 \Omega_2 \vec{E}_1 \\ & \times (\nabla \times \vec{E}_2) + \omega_2 \Omega_1 \vec{E}_2 \times (\nabla \times \vec{E}_1) \}. \end{aligned} \quad (10)$$

At this point we will concentrate only on the nonlinear response of the selvedge and we will consider the nonlinear bulk response later. The width of the selvedge can be safely assumed to be much smaller than the wavelength. Hence, we ignore retardation, i.e., we drop $\nabla \times \vec{E}_i$ from Eq. (10), and we ignore the slow variation of the field along the surface. Since we are ignoring retardation we can identify the displacement field $D_z = E_z + 4\pi P_z$ with the external field. Due to the absence of an external field at ω_3 , we may substitute E_{3z} by the depolarization field $-4\pi P_{3z}$. We also write $E_{iz}(z) = D_{iz}/\epsilon(\omega_i, z)$ where $\epsilon(\omega_i, z)$ is the dielectric function which we write as

$$\epsilon(\omega_i, z) \equiv \epsilon_i(z) = 1 - \frac{4\pi e^2/m}{\omega_i \Omega_i} n(z), \quad (11)$$

where $i=1,2,3$, and D_{iz} is a slowly varying function of z . We ignore spatial dispersion effects, which are expected to

be important close to the surface where the field E_{iz} has its most abrupt variations. Making use of the long-wavelength approximation (LWA) we assume that the displacement field D_{iz} is constant across the surface region, and we solve Eq. (10) for P_{3z} to obtain

$$\begin{aligned} P_{3z}(z) = & \frac{1}{\epsilon_3(z)} \left[-\frac{e^3/m^2}{\omega_3 \Omega_3} n_0(z) \right. \\ & \times \left(\frac{1}{\omega_1 \Omega_1} \frac{1}{\epsilon_1(z)} \frac{\partial}{\partial z} \frac{1}{\epsilon_2(z)} + 1 \leftrightarrow 2 \right) \\ & + \left. \frac{e^3/m^2}{\omega_1 \omega_2 \Omega_1 \Omega_2} \frac{\partial}{\partial z} n_0(z) \frac{1}{\epsilon_1(z)} \frac{1}{\epsilon_2(z)} \right] D_{1z} D_{2z}, \end{aligned} \quad (12)$$

where $1 \leftrightarrow 2$ denotes the previous terms transposing the indices 1 and 2. The SF polarization given above depends on z through $n_0(z)$ and its spatial derivative [see Eq. (11)] which vanishes in both vacuum and bulk. Therefore, P_{3z} is different from zero only in the selvedge region. Following the LWA, we characterize the polarization at the surface by its zeroth moment

$$\vec{P}_3 \equiv \int_{-\infty}^{\infty} dz \vec{P}_3(z). \quad (13)$$

Substituting Eq. (12) we obtain terms of the form $\int dz f(n_0(z)) dg(n_0(z))/dz$ where f and g are simply rational functions of the density profile $n_0(z)$. We divide the integration range into intervals so that in each of them n_0 is monotonic, and we can change the integration variable $z \rightarrow n_0$ employing $dz = dn_0/(dn_0/dz)$ and $dg(n_0(z))/dz = (dn_0/dz)(dg/dn_0)$. It is easily seen that dn_0/dz cancels out from the integral so that we are left with integrals in dn_0 of rational functions of n_0 . These integrals are now evaluated from $n_0(z \rightarrow -\infty) = 0$ to $n_0(z \rightarrow \infty) = n_B$, with n_B the bulk value of the density, and they can be performed analytically for any profile $n_0(z)$ yielding

$$P_{3z} = \chi_{zzz}^s(\omega_1, \omega_2) D_{1z} D_{2z} + 1 \leftrightarrow 2. \quad (14)$$

Notice that our definition of χ^s is explicitly symmetrized in the frequencies ω_1, ω_2 . As $\chi_{ijk}^s(\omega_1, \omega_2) = \chi_{ikj}^s(\omega_2, \omega_1)$, this symmetrization is sometimes omitted,¹⁴ yielding twice our surface susceptibility. It is convenient to write the resulting surface susceptibility χ_{zzz}^s in terms of phenomenological dimensionless parameter $a(\omega_1, \omega_2)$

$$\chi_{zzz}^s(\omega_1, \omega_2) = \frac{-1}{64\pi^2 n_B e} \frac{\omega_p^4}{\omega_1 \omega_2 \Omega_1 \Omega_2} \frac{1}{\epsilon_1 \epsilon_2} a(\omega_1, \omega_2), \quad (15)$$

from where we obtain

$$a(\omega_1, \omega_2) = -2 \frac{\left[\left(\frac{1}{\omega_1 \Omega_1} - \frac{1}{\omega_2 \Omega_2} \right) \epsilon_1 \epsilon_2 + \text{c.p.} \right] + \frac{1}{\omega_3 \Omega_3} \epsilon_1 \epsilon_2 \left[\epsilon_2 \log \left(\frac{\epsilon_3}{\epsilon_1} \right) + \text{c.p.} \right]}{\omega_p^4 \left(\frac{1}{\omega_1 \Omega_1} - \frac{1}{\omega_3 \Omega_3} \right) \left(\frac{1}{\omega_3 \Omega_3} - \frac{1}{\omega_2 \Omega_2} \right) \left(\frac{1}{\omega_2 \Omega_2} - \frac{1}{\omega_1 \Omega_1} \right)}, \quad (16)$$

where c.p. denotes a sum over cyclic permutations of the indices (1,2,3) and $\epsilon_i = 1 - \omega_p^2/\omega_i\Omega_i$ without an explicit z dependence denotes the bulk dielectric function, with $\omega_p = \sqrt{4\pi e^2 n_B/m}$, the bulk plasma frequency. We remark that due to our neglect of spatial dispersion the resulting nonlinear surface susceptibility (15) is *independent of the density profile* $n_0(z)$ and depends only on its bulk value n_B . Therefore, Eq. (15) yields an unambiguous well defined result^{18,17} even in the unrealistic extreme case of an discontinuous abrupt surface.

It can be easily verified that our expression (16) agrees with the quantum-mechanical result¹⁹ in the high-frequency limit $a(\omega_1 \rightarrow \infty, \omega_2 \rightarrow \infty) = a(\omega_1 \rightarrow \infty, \omega_2) = a(\omega_1, \omega_2 \rightarrow \infty) = -2$ first derived for SHG. This limit is a test to which calculations ought to be subjected. However, the low frequency limit of Eq. (16) diverges. This result is unrealistic, as more sophisticated models yield a finite value for the static limit of a .^{14,20} The reason for this failure is our neglect of spatial dispersion within the present model. This omission is particularly important at the surface of conductors when the driving fields and the response of the system are perpendicular to the surface. On the other hand, the results obtained below for the other components of the surface susceptibility are indeed correct for the jellium model.

By considering the parallel component of the polarization, we now get

$$\vec{P}_{3\parallel}(z) = \frac{e^3/m^2}{\omega_1\omega_2\Omega_1\Omega_2} \frac{\omega_1}{\omega_3} \frac{\partial n_0(z)}{\partial z} \vec{E}_{1\parallel} D_{2z} + 1 \leftrightarrow 2, \quad (17)$$

in a similar way as we obtained Eq. (12) from Eq. (10). Here, we have also ignored the first term of Eq. (10), as the non-retarded depolarization field parallel to the surface is null. Integrating this equation across the surface [Eq. (13)] we obtain

$$\vec{P}_{3\parallel} = \chi_{\parallel\parallel z}^s(\omega_1, \omega_2) \vec{E}_{1\parallel} D_{2z} + \chi_{\parallel\parallel z}^s(\omega_1, \omega_2) D_{1z} \vec{E}_{2\parallel} + 1 \leftrightarrow 2. \quad (18)$$

As with the perpendicular component of the SF polarization, we parameterize the surface susceptibility as

$$\begin{aligned} \chi_{\parallel\parallel z}^s(\omega_1, \omega_2) &= \chi_{\parallel\parallel z}^s(\omega_2, \omega_1) \\ &= \frac{-1}{64\pi^2 n_B e} \frac{\omega_p^4}{\omega_1\omega_2\Omega_1\Omega_2} \frac{1}{\epsilon_2} \frac{2\omega_1}{\omega_3} b(\omega_1, \omega_2), \end{aligned} \quad (19a)$$

$$\begin{aligned} \chi_{\parallel\parallel z}^s(\omega_2, \omega_1) &= \chi_{\parallel\parallel z}^s(\omega_1, \omega_2) \\ &= \frac{-1}{64\pi^2 n_B e} \frac{\omega_p^4}{\omega_1\omega_2\Omega_1\Omega_2} \frac{1}{\epsilon_1} \frac{2\omega_2}{\omega_3} b(\omega_2, \omega_1), \end{aligned} \quad (19b)$$

in terms of the dimensionless parameters $b(\omega_1, \omega_2)$ and $b(\omega_2, \omega_1)$, which are given by

$$b(\omega_1, \omega_2) = b(\omega_2, \omega_1) = -1 \quad (20)$$

in our particular model. Since our system is homogeneous along the surface, the only component of the electric field that has a large gradient is that normal to the surface. There-

fore, if the driving field is parallel to the surface there is no surface polarization and so, $\chi_{z\parallel\parallel}^s = 0$. The other components of the surface susceptibility are null¹⁴ due to the rotational and in-plane inversion symmetry of the flat interface.

We remark that we have defined the different components of the surface susceptibility in terms of field components D_{iz} and $E_{i\parallel}$ which are continuous at abrupt surfaces and which are slowly varying across smooth interfaces.^{18,21,22} This allows us to employ the LWA and makes it unnecessary to specify the position near the surface where the fields are to be evaluated, therefore eliminating a source of confusion in the literature. We also remark that the surface susceptibility yields the self-consistent, total surface polarization, so that it should not be further screened, i.e., it may be situated outside of the metal when employed in radiated field calculations.

Now we turn our attention to the bulk nonlinear response. We write¹⁴

$$\vec{E}_i(\vec{r}) = \vec{E}_i e^{i\vec{q}_i \cdot \vec{r}}, \quad (21)$$

where the bulk wave vectors of the fundamental normal modes are $\vec{q}_i = (\vec{q}_{i\parallel}, q_{iz})$ ($i=1,2$), $\vec{q}_{i\parallel}$ is determined by the incident field, i.e., $q_{i\parallel} = (\omega_i/c)\sin(\theta_i)$ with θ_i the angle of incidence of the i th beam, and q_{iz} solves the bulk dispersion relation, i.e., $q_{iz}^2 = (\omega_i/c)^2 \epsilon_i - q_{i\parallel}^2$. Substituting Eq. (21) into Eq. (10) we get, straightforwardly,

$$\vec{P}_3^B(\vec{r}) = i e^{i(\vec{q}_1 + \vec{q}_2) \cdot \vec{r}} [D_1 \vec{q}_1 (\vec{E}_1 \cdot \vec{E}_2) + \bar{D}_1 (\vec{q}_1 \cdot \vec{E}_2) \vec{E}_1 + 1 \leftrightarrow 2], \quad (22)$$

without neglecting retardation. It should be noted that we dropped the linear response to the SF field in Eq. (10) so that \vec{P}_3^B is not the total bulk polarization, but only the source of the SF field within the bulk. The bulk response of an isotropic media is characterized by the parameters D_i and \bar{D}_i ,¹⁴ given within our model by

$$D_i = \frac{n_B e^3}{m^2} \frac{\Omega_i}{\omega_3 \Omega_1 \Omega_2 \Omega_3 \omega_i}, \quad (23)$$

and

$$\bar{D}_i = \frac{n_B e^3}{m^2} \frac{1}{\omega_1 \omega_2 \Omega_1 \Omega_2} \left(\frac{\omega_i}{\omega_3} - \frac{\Omega_i}{\Omega_3} \right). \quad (24)$$

It is important to remark that Petukhov¹⁴ has also developed a hydrodynamic model and has obtained results similar to the present ones. However, he concluded that $\bar{D}_i = 0$ identically. Here, we see that the vanishing of \bar{D}_i is not a generic result, but is a consequence of having neglected dissipation. This can be easily verified by setting $\tau = \infty$, which implies $\Omega_i = \omega_i$, in Eq. (24).

B. Continuous dipolium model of dielectrics

In the present subsection we present a model for the nonlinear response of dielectric materials, closely following that developed previously¹⁶ for SHG.

We start by considering a single polarizable entity within a dielectric material. We model the entity by an electron with charge $-e$ and mass m at a distance \vec{x} from its equilibrium

position, to which it is bound by a harmonic force with resonant frequency ω_0 . In the presence a spatially varying electromagnetic field $\vec{E}(\vec{r}, t)$ and $\vec{B}(\vec{r}, t)$ its classical equation of motion is

$$m\ddot{\vec{x}} = -e\vec{E} - m\omega_0^2\vec{x} - \frac{m}{\tau}\dot{\vec{x}} - \frac{e}{c}\dot{\vec{x}} \times \vec{B}, \quad (25)$$

where we also added a dissipative term with corresponding lifetime τ . We notice that, in this equation, the field has to be evaluated at the actual position of the electron, $\vec{r}_0 + \vec{x}$, and not simply at its equilibrium position \vec{r}_0 . Therefore, assuming that the scale of variation of the polarizing electric field is not smaller than the expectation value \vec{x} , we carry out a Taylor expansion to first order as

$$\vec{E}(\vec{r}_0 + \vec{x}, t) \approx \vec{E}(\vec{r}_0, t) + \vec{x} \cdot \nabla \vec{E}(\vec{r}_0, t) + \dots \quad (26)$$

and we make a similar expansion to zeroth-order for the magnetic interaction. Higher-order terms in these expansions would have no effect in the quadratic nonlinear response studied below. Thus, substituting Eq. (26) the equation of motion (25) becomes

$$m\ddot{\vec{x}} = -e\vec{E}(\vec{r}_0, t) - m\omega_0^2\vec{x} - \frac{m}{\tau}\dot{\vec{x}} - e\vec{x} \cdot \nabla \vec{E}(\vec{r}_0, t) - \frac{e}{c}\dot{\vec{x}} \times \vec{B}(\vec{r}_0, t) + \dots \quad (27)$$

This is similar to the equation of a forced harmonic oscillator: it has a driving term $-eE$ and all the other terms are proportional to the displacement \vec{x} . However, the coefficients of \vec{x} and $d\vec{x}/dt$ in the last two terms are field dependent, and, therefore, time dependent, giving rise to a nonlinearity similar to that of a parametric, forced oscillator. Notice that, apparently, there is a substantial difference in the source of nonlinearity of this and the previous model developed in Sec. II A. Here we made a Taylor expansion of the field around the equilibrium position of the charge; while there, we followed the motion of a charged fluid and used the nonlinear convective time derivative. This difference is analogous to that usually found in fluid dynamics, where the position of a fluid element may be described in terms of Eulerian or Lagrangian coordinates.²³

Now we assume that the driving fields are two monochromatic waves with frequency ω_1 and ω_2 , and, since optical fields are usually much smaller than atomic fields, we proceed to a perturbative solution of Eq. (27) by expanding its solution in powers of \vec{E} ,

$$\vec{x}(t) = \vec{x}^{(1)}(t) + \vec{x}^{(2)}(t) + \dots \quad (28)$$

The lowest-order solution is a superposition of two monochromatic waves with amplitudes $\vec{x}_1^{(1)} \equiv \vec{x}^{(1)}(\omega_1)$ and $\vec{x}_2^{(1)} \equiv \vec{x}^{(1)}(\omega_2)$ corresponding to each frequency ω_1 and ω_2 , from which we find the induced electric dipole moment $\vec{p}_i^{(1)} = -e\vec{x}_i^{(1)} = \alpha(\omega_i)\vec{E}_i$, $i = 1, 2$, where the linear polarizability is

$$\alpha_i \equiv \alpha(\omega_i) = \frac{e^2/m}{\omega_0^2 - \omega_i^2 - i\omega_i/\tau}. \quad (29)$$

The second-order equation,

$$m\ddot{\vec{x}}^{(2)}(t) = -m\omega_0^2\vec{x}^{(2)}(t) - \frac{m}{\tau}\dot{\vec{x}}^{(2)}(t) - e\vec{x}^{(1)}(t) \cdot \nabla \vec{E}(\vec{r}_0, t) - \frac{e}{c}\dot{\vec{x}}^{(1)}(t) \times \vec{B}(\vec{r}_0, t), \quad (30)$$

is linear in $\vec{x}^{(2)}$ and has a driving term that is quadratic in \vec{E} with five frequency components: a dc contribution, and four oscillatory terms at $2\omega_1$, $2\omega_2$, $\omega_1 - \omega_2$, and $\omega_1 + \omega_2$. They correspond to optical rectification, second harmonic of ω_1 and ω_2 , difference frequency generation, and sum frequency generation, respectively. We look now for the SFG component of $\vec{x}^{(2)}$, $\vec{x}_3^{(2)} \equiv \vec{x}^{(2)}(\omega_3)$, which obeys

$$\omega_3^2\vec{x}_3^{(2)} = \omega_0^2\vec{x}_3^{(2)} - i\frac{\omega_3}{\tau}\vec{x}_3^{(2)} + \frac{e}{m}(\vec{x}_1^{(1)} \cdot \nabla \vec{E}_2 + \vec{x}_2^{(1)} \cdot \nabla \vec{E}_1) - \frac{e}{m} \left(\frac{\omega_1}{\omega_2} \vec{x}_1^{(1)} \times \nabla \times \vec{E}_2 + \frac{\omega_2}{\omega_1} \vec{x}_2^{(1)} \times \nabla \times \vec{E}_1 \right), \quad (31)$$

where we wrote each monochromatic component of the magnetic field in terms of the curl of the corresponding electric field. The solution of Eq. (31) gives the induced nonlinear SF dipole moment $\vec{p}_3^{(2)} = -e\vec{x}_3^{(2)}$ as

$$\begin{aligned} \vec{p}_3^{(2)} &\equiv \vec{p}^{(2)}(\omega_3) \\ &= -\frac{1}{e}\alpha_3 \left[\alpha_1 \left(\vec{E}_1 \cdot \nabla \vec{E}_2 - \frac{\omega_1}{\omega_2} \vec{E}_1 \times (\nabla \times \vec{E}_2) \right) \right. \\ &\quad \left. + \alpha_2 \left(\vec{E}_2 \cdot \nabla \vec{E}_1 - \frac{\omega_2}{\omega_1} \vec{E}_2 \times (\nabla \times \vec{E}_1) \right) \right]. \end{aligned} \quad (32)$$

Finally, there are two other moments of second order in the driving field that oscillate with frequency ω_3 : one is the familiar electric quadrupole moment $\vec{Q}^{(2)}(\omega_3) = -e\vec{x}_1^{(1)}\vec{x}_2^{(1)} + 1 \leftrightarrow 2$, which is simply given by

$$\vec{Q}_3^{(2)} \equiv \vec{Q}^{(2)}(\omega_3) = -\frac{1}{e}\alpha_1\alpha_2(\vec{E}_1\vec{E}_2 + \vec{E}_2\vec{E}_1). \quad (33)$$

The other is the magnetic-dipole moment $\vec{\mu}$ given by

$$\vec{\mu} = \frac{-e}{2mc}\dot{\vec{x}} \times m\dot{\vec{x}}. \quad (34)$$

We remark that this contribution has been ignored in second-order optically related surface susceptibility calculations. The SF component turns out to be

$$\begin{aligned}
\vec{\mu}_3^{(2)} \equiv \vec{\mu}^{(2)}(\omega_3) &= -\frac{e}{2c} [\vec{x}_1^{(1)} \times \dot{\vec{x}}_2^{(1)} + \vec{x}_2^{(1)} \times \dot{\vec{x}}_1^{(1)}] \\
&= \frac{i}{2ce} \alpha_1 \alpha_2 [\omega_2 \vec{E}_1 \times \vec{E}_2 + \omega_1 \vec{E}_2 \times \vec{E}_1] \\
&= \frac{i}{2ce} \alpha_1 \alpha_2 (\omega_2 - \omega_1) \vec{E}_1 \times \vec{E}_2.
\end{aligned} \tag{35}$$

We stress that this term is zero for the usual SHG (Ref. 24) as well as for noncollinear SHG where there are two fundamental beams at different angles of incidence. We also remark that although this is a magnetic term, it is driven by the linear electric fields. An example of a magnetic effect induced by an electric field is the reciprocal of the Faraday effect, i.e., the dc magnetization induced by a circularly polarized electromagnetic wave.²⁵ This effect is described by Eq. (35), as can be simply verified by setting $\omega_2 = -\omega_1$ and $\vec{E}_2 = \vec{E}_1^*$.

As in the case of linear response and of SHG,²⁶ the nonlinear response functions of a harmonic oscillator which we have derived above classically, coincide with the corresponding expressions derived from a full quantum-mechanical calculation. As in the case of SHG and in analogy to Miller's rule²⁷⁻²⁹ for the bulk nonlinear response of noncentrosymmetric systems, we conjecture that the corrections to Eqs. (32) and (33) in centrosymmetric molecules that are not harmonic oscillators might turn out to be small and with only a slow frequency dependence.

Now we consider a macroscopic semi-infinite system made up of n polarizable entities per unit volume, and we will allow $n = n(z)$ to depend on position, changing rapidly, but continuously near the surface $z=0$ from its bulk value $n(z \rightarrow \infty) = n_B$ to its vacuum value $n(z \rightarrow -\infty) = 0$. Each entity occupies a different position, which we will denote by \vec{r} and we will assume that \vec{r} is a continuous variable. Thus, in the following, we will ignore effects derived from the microscopic crystalline structure of the system. We will also assume the response of each entity to be independent of \vec{r} , so that we will also neglect effects such as those derived from a surface induced modification to the electronic structure. Therefore, we will concentrate our attention only on the contribution of the spatial variation of the electromagnetic field on the sum frequency generation.

We begin by writing the macroscopic second order polarization \vec{P}_3 as³⁰

$$\vec{P}_3(z) = n(z) \vec{p}_3^{(2)} - \frac{1}{2} \nabla \cdot n(z) \vec{Q}_3^{(2)} + \frac{ic}{\omega_3} \nabla \times n(z) \vec{\mu}_3^{(2)}, \tag{36}$$

where \vec{P}_3 , $\vec{p}_3^{(2)}$, $\vec{Q}_3^{(2)}$, and $\vec{\mu}_3^{(2)}$ are continuously varying functions of \vec{r} .³¹ At this point we are interested only in the nonlinear response of the selvedge; the bulk response will be considered later. To get the selvedge response we neglect retardation and the slow spatial variations of the field as before, and approximate

$$\begin{aligned}
\vec{P}_3 &= n(z) \alpha_3 \vec{E}_3 - \frac{n(z)}{e} \alpha_3 (\alpha_1 \vec{E}_1 \cdot \nabla \vec{E}_2 + \alpha_2 \vec{E}_2 \cdot \nabla \vec{E}_1) \\
&\quad + \frac{1}{2e} \alpha_1 \alpha_2 \nabla \cdot n(z) (\vec{E}_1 \vec{E}_2 + \vec{E}_2 \vec{E}_1) \\
&\quad - \frac{1}{2e} \alpha_1 \alpha_2 \left(\frac{\omega_2 - \omega_1}{\omega_3} \right) \nabla \times n(z) (\vec{E}_1 \times \vec{E}_2),
\end{aligned} \tag{37}$$

where the first term on the RHS is the linear response to the SF field $\vec{E}_3 \equiv \vec{E}(\omega_3)$, which we have added for consistency. Again, we notice that the last term of Eq. (37) does not contribute to SHG.

Now, following the same procedure that took us from Eq. (10) to Eq. (14), we solve Eq. (37) to get both the perpendicular and parallel components of the polarization \vec{P}_3 , within the dipolium model for dielectrics. For the perpendicular component we get

$$\begin{aligned}
P_{3z}(z) &= \frac{1}{e \epsilon_3(z)} \left[-n(z) \alpha_3 \right. \\
&\quad \times \left(\alpha_1 \frac{1}{\epsilon_1(z)} \frac{\partial}{\partial z} \frac{1}{\epsilon_2(z)} + \alpha_2 \frac{1}{\epsilon_2(z)} \frac{\partial}{\partial z} \frac{1}{\epsilon_1(z)} \right) \\
&\quad \left. + \alpha_1 \alpha_2 \frac{\partial}{\partial z} n(z) \frac{1}{\epsilon_1(z)} \frac{1}{\epsilon_2(z)} \right] D_{1z} D_{2z} + 1 \leftrightarrow 2.
\end{aligned} \tag{38}$$

Substituting Eq. (38) into Eq. (13) we obtain $P_{3z} = \chi_{zzz}^s(\omega_1, \omega_2) D_{1z} D_{2z} + 1 \leftrightarrow 2$, where in analogy to the previous case, we now write the surface susceptibility in terms of a dimensionless parameter $a(\omega_1, \omega_2)$, through

$$\chi_{zzz}^s(\omega_1, \omega_2) = -\frac{a(\omega_1, \omega_2)}{4n_B e} \frac{\epsilon_1 - 1}{4\pi \epsilon_1} \frac{\epsilon_2 - 1}{4\pi \epsilon_2}, \tag{39}$$

where

$$a(\omega_1, \omega_2) = -2 \left[1 + \frac{(1 - \epsilon_3) \epsilon_1 \epsilon_2 [\epsilon_2 \log(\epsilon_3 / \epsilon_1) + \text{c.p.}]}{(\epsilon_1 - \epsilon_2)(\epsilon_2 - \epsilon_3)(\epsilon_3 - \epsilon_1)} \right]. \tag{40}$$

The bulk dielectric function is now given by $\epsilon_i = 1 + 4\pi n_B \alpha_i$.

We follow a similar procedure for the parallel components of the polarization \vec{P}_3 . Starting from Eq. (37) we obtain, in analogy to Eq. (38),

$$\begin{aligned}
\vec{P}_{3\parallel}(z) &= \frac{1}{2e} \alpha_1 \alpha_2 \left[\vec{E}_{1\parallel} \frac{\partial}{\partial z} \frac{n(z)}{\epsilon_2(z)} D_{2z} + \vec{E}_{2\parallel} \frac{\partial}{\partial z} \frac{n(z)}{\epsilon_1(z)} D_{1z} \right. \\
&\quad \left. - \left(\frac{\omega_2 - \omega_1}{\omega_3} \right) \left(\frac{\partial}{\partial z} \frac{n(z)}{\epsilon_2(z)} D_{2z} \vec{E}_{1\parallel} \right. \right. \\
&\quad \left. \left. - \frac{\partial}{\partial z} \frac{n(z)}{\epsilon_1(z)} D_{1z} \vec{E}_{2\parallel} \right) \right],
\end{aligned} \tag{41}$$

which can be integrated, yielding

$$\begin{aligned}
\vec{\mathcal{P}}_{3\parallel} &= \int_{-\infty}^{\infty} dz \vec{P}_{3\parallel}(z) \\
&= \frac{1}{2e} \alpha_1 \alpha_2 \left[\frac{n_B}{\epsilon_2} \left(1 - \frac{\omega_2 - \omega_1}{\omega_3} \right) \vec{E}_{1\parallel} D_{2z} \right. \\
&\quad \left. + \frac{n_B}{\epsilon_1} \left(1 + \frac{\omega_2 - \omega_1}{\omega_3} \right) \vec{E}_{2\parallel} D_{1z} \right] \\
&\equiv \chi_{\parallel\parallel z}^s(\omega_1, \omega_2) \vec{E}_{1\parallel} D_{2z} + \chi_{\parallel z\parallel}^s(\omega_1, \omega_2) D_{1z} \vec{E}_{2\parallel} + 1 \leftrightarrow 2,
\end{aligned} \tag{42}$$

where the surface susceptibilities are

$$\begin{aligned}
\chi_{\parallel\parallel z}^s(\omega_1, \omega_2) &= \chi_{\parallel z\parallel}^s(\omega_2, \omega_1) \\
&= \frac{-1}{4n_B e} \frac{(\epsilon_1 - 1)(\epsilon_2 - 1)}{(4\pi)^2} \frac{1}{\epsilon_2} \frac{2\omega_1}{\omega_3} b(\omega_1, \omega_2),
\end{aligned} \tag{43a}$$

$$\begin{aligned}
\chi_{\parallel z\parallel}^s(\omega_2, \omega_1) &= \chi_{\parallel\parallel z}^s(\omega_1, \omega_2) \\
&= \frac{-1}{4n_B e} \frac{(\epsilon_1 - 1)(\epsilon_2 - 1)}{(4\pi)^2} \frac{1}{\epsilon_1} \frac{2\omega_2}{\omega_3} b(\omega_2, \omega_1),
\end{aligned} \tag{43b}$$

and

$$b(\omega_1, \omega_2) = b(\omega_2, \omega_1) = -1 \tag{44}$$

as for our model conductor. The other components of the surface susceptibility are null. The susceptibilities above are consistent with those previously obtained for SHG.¹⁶

We may compare the results obtained here for our nonlinear dipolium model with those obtained in the previous subsection for jellium, simply by substituting the Drude dielectric function (11) in Eqs. (39), (40), and (43). Both sets of results agree, as could be expected, since our local jellium can be thought of as a harmonic dipolium with a null restoring force. Not only do the surface susceptibilities are in agreement, but also, the parametrization in terms of a and b employed here agrees with that used for jellium. This shows the convenience of using our expressions (39) and (43) for parametrizing the surface response, as opposed to parametrizations in terms of model-dependent parameters, such as the plasma frequency and the lifetime for jellium. Finally, it should be noted that the agreement between dipolium and jellium results would not have been obtained had we neglected the nonlinear magnetic contribution $\vec{\mu}$ to the polarization in Eq. (36). This illustrates the need of incorporating the electric-driven magnetic-dipole moment in SFG calculations.

Now we turn our attention to the bulk non-linear response for the dielectric case. We substitute Eqs. (32), (33), and (35) into Eq. (36), and we assume that the fundamental fields propagate as plane waves (21) to obtain again Eq. (22), but now with the bulk parameters D_i and \bar{D}_i defined as

$$\begin{aligned}
D_i &= \frac{1}{n_B e} \frac{(\epsilon_3 - 1)}{4\pi} \frac{(\epsilon_1 - 1)}{4\pi} \frac{(\epsilon_2 - 1)}{4\pi} \frac{4\pi}{(\epsilon_i - 1)} \frac{\omega_1 \omega_2}{\omega_i^2} \\
&\equiv \frac{1}{n_B e} \frac{(\epsilon_3 - 1)}{4\pi} \frac{(\epsilon_1 - 1)}{4\pi} \delta_i d_i
\end{aligned} \tag{45a}$$

$$\begin{aligned}
\bar{D}_i &= \frac{1}{n_B e} \left[\frac{(\epsilon_1 - 1)}{4\pi} \frac{(\epsilon_2 - 1)}{4\pi} \frac{\omega_i}{\omega_3} \right. \\
&\quad \left. - \frac{(\epsilon_3 - 1)}{4\pi} \frac{(\epsilon_1 - 1)}{4\pi} \frac{(\epsilon_2 - 1)}{4\pi} \frac{4\pi}{(\epsilon_i - 1)} \frac{\omega_3}{\omega_i} \right] \\
&\equiv \frac{1}{n_B e} \frac{(\epsilon_3 - 1)}{4\pi} \frac{(\epsilon_1 - 1)}{4\pi} \bar{\delta}_i \bar{d}_i,
\end{aligned} \tag{45b}$$

where we have introduced the bulk parameters

$$\delta_i = \frac{\epsilon_3 - 1}{\epsilon_i - 1} \frac{\omega_1 \omega_2}{\omega_i^2}, \tag{46a}$$

$$\bar{\delta}_i = \frac{\omega_i}{\omega_3} - \frac{\epsilon_3 - 1}{\epsilon_i - 1} \frac{\omega_3}{\omega_i}, \tag{46b}$$

so that

$$d_1 = d_2 = \bar{d}_1 = \bar{d}_2 = 1, \tag{47}$$

with $i=1,2$. As before, it is straightforward to verify that when the Drude dielectric function is substituted in Eqs. (45) our bulk parameters agree with those of jellium, Eqs. (23) and (24).

III. RESULTS

In this section we present results for the nonlinear response corresponding to two particular cases. The first is a solid made out of identical harmonic polarizable entities with a single resonance and the second is Si. Having obtained the surface and bulk susceptibilities for our two models of conductors and dielectrics, we proceed to obtain the efficiency of the SF radiation, defined by

$$\mathcal{R}_{\alpha\beta\gamma} = \frac{I_\gamma^{(out)}(\omega_3)}{I_\alpha^{(in)}(\omega_1) I_\beta^{(in)}(\omega_2)}, \tag{48}$$

where $I_\gamma^{(out)}(\omega_3)$ ($I_{\alpha,\beta}^{(in)}(\omega_{1,2})$) denotes the intensity of the outgoing SF (ingoing fundamental) field at ω_3 (ω_1, ω_2) for polarization γ (α, β). Notice that in the limit $\omega_1 \rightarrow \omega_2$ the efficiency (48) yields four times the SH efficiency.¹⁵ The reason simply is that in that limit, the second harmonic polarization is proportional to $(E_1 + E_2)^2$, which has the term $2E_1 E_2$, while in SFG we pick only the term $E_1 E_2$ (without writing explicitly the factor 2!). In the Appendix we follow Ref. 14 to obtain explicit formulas for $\mathcal{R}_{\alpha\beta\gamma}$ in the terms of the surface and bulk parameters a , b , δ , $\bar{\delta}$, d , and \bar{d} . We restrict ourselves to the ppp polarization combination, since this is the most efficient among the different choices.

In Fig. 1 we plot the imaginary part of $a(\omega_1, \omega_2)$ vs the normalized frequency ω_1/ω_0 and ω_2/ω_0 , for a harmonic solid with parameters $n_B = m\omega_0^2/(4\pi e^2)$ and $\omega_0\tau = 20$. We notice that the plot is symmetric with respect to the inter-

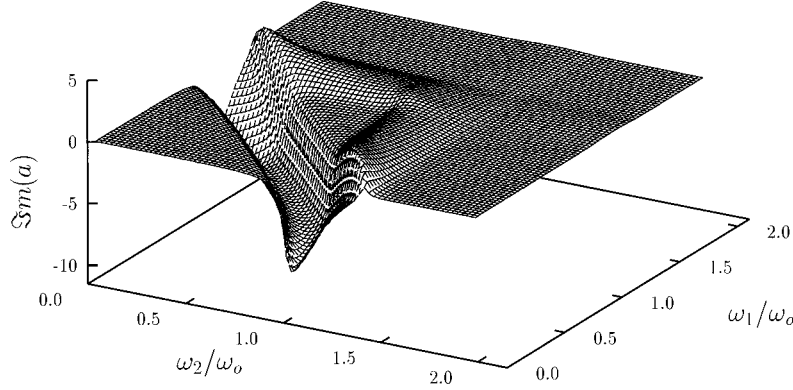


FIG. 1. Imaginary part of $a(\omega_1, \omega_2)$ vs ω_1/ω_0 and ω_2/ω_0 , for a harmonic solid with resonance frequency ω_0 , and lifetime parameter $\tau=20/\omega_0$.

change $\omega_1 \leftrightarrow \omega_2$, a property that is inherited from the symmetry of the surface susceptibility $\chi_{zzz}^s(\omega_1, \omega_2)$ [Eq. (14) and Eq. (15)]. To understand the structure displayed in Fig. 1, we recall that the bulk dielectric function of such a solid $\epsilon(\omega)$ displays a resonance at ω_0 . In the region between the transverse (ω_0) and the longitudinal ($\omega_L = \sqrt{\omega_0^2 + 4\pi n_B e^2/m}$) frequencies, the dielectric function becomes negative and the logarithmic terms of Eq. (40) become large. Then, we may expect a to have structure whenever ω_1 , ω_2 , or ω_3 lie within this region. Indeed, in Fig. 1 we see two wide ridges that run parallel to the ω_1 and ω_2 axes, extending from $\omega_2 = \omega_0$ ($\omega_1 = \omega_0$) up to $\omega_L = \sqrt{2}\omega_0$ and a valley that cuts diagonally from $\omega_1 + \omega_2 = \omega_3 \approx \omega_0$ to ω_L . If we traverse Fig. 1 along the diagonal $\omega_1 = \omega_2$ we obtain the SH response $a_{\text{SH}}(\omega)$, which is identical to our previous result.¹⁶ The real part of a has features in the same regions as the imaginary part, to which it is related by causality relations.

In Fig. 2 we plot \mathcal{R}_{ppp} vs ω_1/ω_0 and ω_2/ω_0 , for the same harmonic system, and for collinear beams at an angle of incidence $\theta_1 = \theta_2 = \theta = 45^\circ$. We remark that the structure of a is strongly suppressed by the Fresnel factors below ω_0 and is much smaller than that apparent above ω_0 . The features that are present correspond to the regions between ω_0 and ω_L where the material is opaque, and also between ω_L and $\omega_c = \sqrt{\omega_L^2/\cos^2\theta - \omega_0^2 \tan^2\theta} \approx 1.73\omega_0$, where there is total internal reflection. There are features whenever ω_1 , ω_2 , or ω_3 are in this region. The structure is enhanced where two ridges cross, and, in particular, the efficiency is maximum where both ω_1 and ω_2 are at resonance with ω_0 . The plot of \mathcal{R}_{ppp} is symmetric with respect to the diagonal $\omega_1 = \omega_2$, and

the corresponding value for $\mathcal{R}_{ppp}(\omega_1 = \omega_2)$ is four times the value of \mathcal{R}_{pp} for SHG,¹⁶ as explained after Eq. (48).

In Fig. 3 we show the p -polarized SF efficiency \mathcal{R}_{ppp} vs ω_1 and ω_2 for two p -polarized beams that incide on a Si surface at angles $\theta_1 = 55^\circ$, and $\theta_2 = 65^\circ$. This was obtained from the formulas of the previous section by simply substituting the experimentally obtained³² dielectric function of bulk Si. As for the harmonic case, we find a similar structure of ridges corresponding to constant values of ω_1 , ω_2 , or ω_3 and peaks where these ridges cross each other. In this case, these structures appear at the frequencies of the critical points of the joint density of states of Si, E_0 , and E_1 .

In Fig. 4 we show \mathcal{R}_{ppp} as a function of the sum frequency ω_3 for a fixed value of one of the fundamentals, ω_1 . Notice that for frequencies $\omega_3 < \omega_1$ we are actually in the DFG and not the SFG regime. However, we can apply our formulas by simply introducing negative frequencies and using the fact that $\alpha(-\omega) = \alpha^*(\omega)$. As expected, the curve displays peaks whenever ω_2 or ω_3 coincide with E_0 or E_1 . As ω_1 diminishes, these peaks overlap and enhance each other. Actually, the peaks at $\omega_3 = E_0$ and E_1 have been observed by Daum *et al.*¹³ by SFG with $\hbar\omega_1 = 2.33$ eV, who also observed the former peak with SHG.^{33–37} Our prediction is that the relative strength of the SFG peaks would be intensified by choosing a lower ω_1 .

As shown in the Appendix, the SFG efficiency may be written as $\mathcal{R}_{\alpha\beta\gamma} \propto |\mathcal{A} + \mathcal{B} + \mathcal{D}|^2$ where \mathcal{A} , \mathcal{B} , and \mathcal{D} are functions of the frequencies and angles which characterize the contributions to the radiation from the surface polarization perpendicular to the surface, parallel to the surface, and the

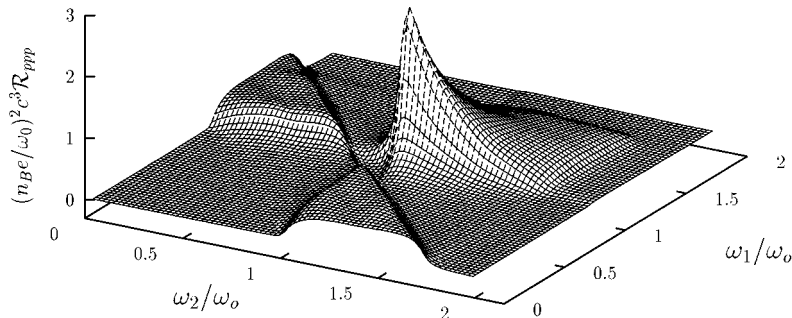


FIG. 2. SF efficiency $(n_B e / \omega_0)^2 c^3 \mathcal{R}_{ppp}$ vs ω_1/ω_0 and ω_2/ω_0 , for the same system as in Fig. 1. The angles of incidence are $\theta_1 = \theta_2 = 45^\circ$.

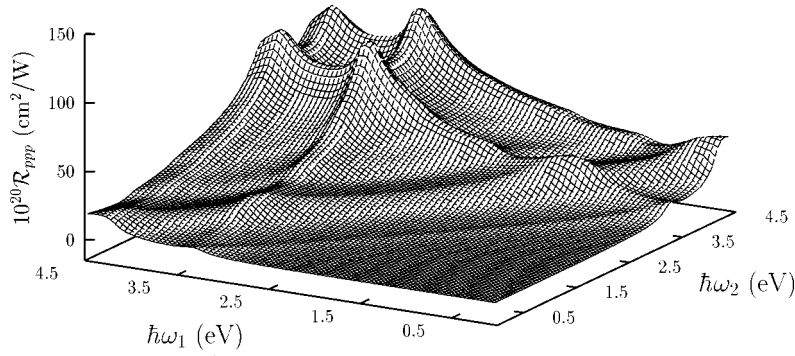


FIG. 3. The vertical axis shows the SF efficiency $10^{20}\mathcal{R}_{ppp}$ (cm²/W) vs ω_1 and ω_2 , for Si. The angles of incidence are $\theta_1=55^\circ$ and $\theta_2=65^\circ$.

bulk contribution, respectively. In Fig. 5 we show the imaginary parts of these three contributions as a function of the sum frequency for a fixed $\hbar\omega_1=0.125$ eV (Ref. 12) corresponding to the solid line of Fig. 4. We see that the largest contribution to the radiated energy comes from the surface polarization normal to the surface. A similar conclusion is obtained from the real parts of \mathcal{A} , \mathcal{B} , and \mathcal{D} .

IV. CONCLUSIONS

We have solved the equations of motion for the electrons in semi-infinite homogeneous centrosymmetric system taking into account the spatial variation of the electromagnetic field, and we have been able to obtain analytic expressions for the surface and bulk nonlinear susceptibilities that describe the process of sum frequency generation. We have defined the surface susceptibilities as the response of the self-consistent total surface polarization to the slowly varying field components. This choice eliminates the usual ambiguities in the position at which the surface fields are to be evaluated and in the choice of position and screening of the surface polarization layer when calculating the radiated field. Furthermore, we have obtained expressions for the conversion efficiency.

We obtained the susceptibilities for both, a system of free electrons (jellium) and a system of polarizable harmonic entities (dipolium) distributed with a number density that varies rapidly but continuously across the surface. These results

were written in terms of the bulk linear dielectric function of the system and dimensionless parameters, and they are independent of the shape of the density profile. This fact allows us to make quantitative calculations of the SFG spectra of arbitrary centrosymmetric systems by simply substituting the appropriate response function, without having to make *ad hoc* assumptions about the density profiles. The dipolium results agree with those for local jellium, but only if a novel term is included in the former, namely, the electric-field-induced nonlinear magnetization. Its contribution to the polarization vanishes in the degenerate case of SHG but is finite for SFG. A comparison between our results for jellium and those previously obtained by Petukhov¹⁴ shows that some components of the bulk susceptibility vanished fortuitously in Ref. 14 and are not zero in general. We have calculated the response and nonlinear efficiency of a harmonic solid and identified its main SFG spectral features in terms of the relevant frequencies of the system, i.e., the resonant, longitudinal, and critical frequencies. We have also applied our results to Si, obtaining features that correspond to its critical points E_0 and E_1 , in qualitative agreement with experiment.¹³ We have shown that these features are intensified as one of the fundamental frequencies goes into the infrared, and that the main contribution to them comes from the surface polarization normal to the surface. We did not present numerical results for local jellium, as it is known that spatial dispersion is very important at conductor surfaces.

In conclusion, we have developed a model that permits

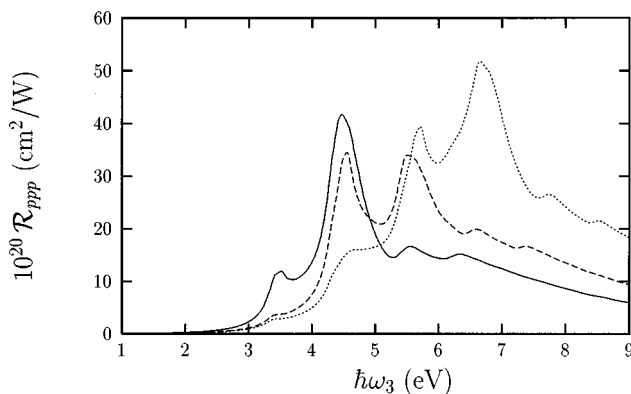


FIG. 4. SF efficiency \mathcal{R}_{ppp} (cm²/W) vs ω_3 for fixed $\hbar\omega_1=0.125$ eV (solid line), $\hbar\omega_1=1.17$ eV (dashed line), and $\hbar\omega_1=2.33$ eV (dotted line), for Si. The angles of incidence are $\theta_1=55^\circ$ and $\theta_2=65^\circ$.

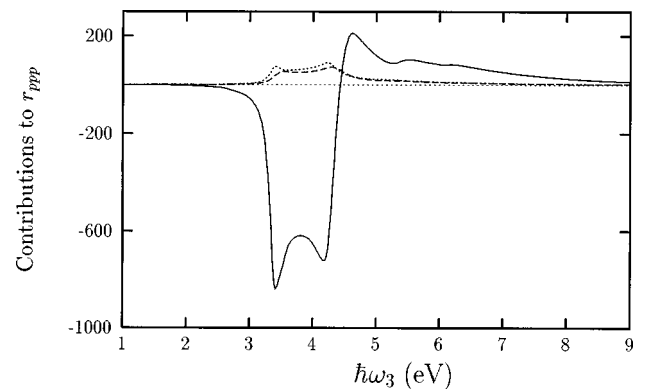


FIG. 5. Plot of the imaginary part of the factors \mathcal{A} (solid line), \mathcal{B} (dashed line), and \mathcal{D} (dotted line) vs ω_3 for fixed $\hbar\omega_1=0.125$ eV, corresponding to the SF efficiency given by the solid line of Fig. 4. See text for details.

calculations of the SFG spectra of arbitrary isotropic centrosymmetric systems. In our model, the surface contribution to SFG arises only from the strong field gradient, that is, we account for the effect of a noncentrosymmetric environment on centrosymmetric molecules. For these reason, the only surface characteristic that enters our model is the number density. However, as we essentially integrated a gradient to obtain the total selvedge contributions, our results turn out to be independent of the density profile, losing surface sensitivity. Nevertheless, there are other surface contributions, such as those arising from the reduction in the symmetry of the wave functions themselves at the surface and from the possible transitions to and from surface states,^{38,39} that should be incorporated in more sophisticated microscopic models, as well as spatial dispersion, crystallinity, and local-field effects.^{40,26,41-44} As sum frequency spectroscopy is rapidly becoming a very powerful probe for surface science, its development requires a more profound theoretical comprehension. This paper represents a step towards this goal.

ACKNOWLEDGMENTS

We are very grateful for illuminating discussions with Vera Brudny and Andrei Petukhov, and we acknowledge the partial support of CONACyT-México 3246-E9308 (B.S.M.) and of DGAPA-UNAM (Grant Nos. IN107796 and IN104594) (W.L.M.).

APPENDIX: RADIATION EFFICIENCY

In this appendix we follow Ref. 14 to calculate the radiated SFG efficiency $\mathcal{R}_{\alpha\beta\gamma}$ [Eq. (48)]. It is convenient to first rewrite the surface and bulk SF polarization in the parametrized fashion,

$$\mathcal{P}_{3z} = \frac{-1}{2n_B e} \left(\frac{\epsilon_1 - 1}{4\pi} \right) \left(\frac{\epsilon_2 - 1}{4\pi} \right) a(\omega_1, \omega_2) \frac{D_{1z}}{\epsilon_1} \frac{D_{2z}}{\epsilon_2}, \quad (\text{A1})$$

$$\begin{aligned} \vec{\mathcal{P}}_{3\parallel} = & \frac{-1}{2n_B e} \left(\frac{\epsilon_1 - 1}{4\pi} \right) \left(\frac{\epsilon_2 - 1}{4\pi} \right) \left(b(\omega_1, \omega_2) \vec{E}_{1\parallel} \frac{D_{2z}}{\epsilon_2} \frac{2\omega_1}{\omega_3} \right. \\ & \left. + b(\omega_2, \omega_1) \vec{E}_{2\parallel} \frac{D_{1z}}{\epsilon_1} \frac{2\omega_2}{\omega_3} \right), \quad (\text{A2}) \end{aligned}$$

and

$$\begin{aligned} \vec{\mathcal{P}}_3^B = & \frac{1}{n_B e} \left(\frac{\epsilon_1 - 1}{4\pi} \right) \left(\frac{\epsilon_2 - 1}{4\pi} \right) [\delta_1 d_1 \vec{q}_1 (\vec{E}_1 \cdot \vec{E}_2) \\ & + \delta_2 d_2 \vec{q}_2 (\vec{E}_1 \cdot \vec{E}_2) + \bar{\delta}_1 \bar{d}_1 \vec{E}_1 (\vec{q}_1 \cdot \vec{E}_2) \\ & + \bar{\delta}_2 \bar{d}_2 \vec{E}_2 (\vec{q}_2 \cdot \vec{E}_1)] i e^{i(\vec{q}_1 + \vec{q}_2) \cdot \vec{r}}. \quad (\text{A3}) \end{aligned}$$

It is now a simple matter to substitute the polarization above into the expressions given in Sec. II of Ref. 14 to obtain

$$\mathcal{R}_{\alpha\beta\gamma} = \frac{2\pi^3 \omega_3^2}{(n_B e)^2 c^3} |A_{\alpha\beta\gamma} r_{\alpha\beta\gamma}|^2 \quad (\text{no summation}), \quad (\text{A4})$$

where

$$A_{\alpha\beta\gamma} = \left(\frac{\epsilon_1 - 1}{4\pi} \right) \left(\frac{\epsilon_2 - 1}{4\pi} \right) \frac{F_\alpha(\omega_1) F_\beta(\omega_2) F_\gamma(\omega_3)}{\cos \theta_3}. \quad (\text{A5})$$

Here, the first two indices denote the polarization (*s* or *p*) of the incoming fundamental beams, and the last index corresponds to the polarization of the outgoing SF beam, the F 's are the corresponding Fresnel factors given below. The only nonzero elements of $r_{\alpha\beta\gamma}$ are r_{ppp} , r_{ssp} , r_{pss} , and r_{sps} . The former is given by

$$r_{ppp} = \mathcal{A} + \mathcal{B} + \mathcal{D}, \quad (\text{A6})$$

with

$$\mathcal{A} = \sin \theta_1 \sin \theta_2 \sin \theta_3 \epsilon_3 a(\omega_1, \omega_2), \quad (\text{A7})$$

$$\begin{aligned} \mathcal{B} = & - \left(s_1 s_3 \sin \theta_2 b(\omega_1, \omega_2) \frac{2\omega_1}{\omega_3} \right. \\ & \left. + s_2 s_3 \sin \theta_1 b(\omega_2, \omega_1) \frac{2\omega_2}{\omega_3} \right), \quad (\text{A8}) \end{aligned}$$

$$\begin{aligned} \mathcal{D} = & 2 \left[(\delta_1 d_1 + \delta_2 d_2) \frac{\omega_1 \omega_2}{\omega_3^2} \frac{V^2}{\epsilon'} + \left(\frac{\epsilon_1 \omega_1^2}{\epsilon' \omega_3^2} \delta_1 d_1 \right. \right. \\ & \left. \left. + \frac{\epsilon_2 \omega_2^2}{\epsilon' \omega_3^2} \delta_2 d_2 \right) V - (\bar{\delta}_1 \bar{d}_1 + \bar{\delta}_2 \bar{d}_2) \frac{\omega_1 \omega_2}{\omega_3^2} \frac{W^2}{\epsilon'} \right] \sin \theta_3 \\ & + 2 \gamma \frac{W}{\epsilon'} \left[(\delta_2 d_2 - \delta_1 d_1 + \bar{\delta}_2 \bar{d}_2 - \bar{\delta}_1 \bar{d}_1) \frac{\omega_1 \omega_2}{\omega_3^2} V \right. \\ & \left. - \bar{\delta}_1 \bar{d}_1 \frac{\omega_1^2}{\omega_3^2} \epsilon_1 + \bar{\delta}_2 \bar{d}_2 \frac{\omega_2^2}{\omega_3^2} \epsilon_2 \right], \quad (\text{A9}) \end{aligned}$$

where \mathcal{A} , \mathcal{B} , and \mathcal{D} characterize the contributions to the radiation from the surface polarization perpendicular to the surface, parallel to the surface, and the bulk contribution, respectively. The other non-null terms of $r_{\alpha\beta\gamma}$ are

$$\begin{aligned} r_{ssp} = & 2 \left[(\delta_1 d_1 + \delta_2 d_2) \frac{\omega_1 \omega_2}{\omega_3^2} \frac{V}{\epsilon'} + \delta_1 d_1 \frac{\omega_1^2}{\omega_3^2} \frac{\epsilon_1}{\epsilon'} \right. \\ & \left. + \delta_2 d_2 \frac{\omega_2^2}{\omega_3^2} \frac{\epsilon_2}{\epsilon'} \right] \sin \theta_3 + 2 \gamma (\delta_2 d_2 - \delta_1 d_1) \frac{\omega_1 \omega_2}{\omega_3^2} \frac{W}{\epsilon'}, \quad (\text{A10}) \end{aligned}$$

$$r_{pss} = \sin \theta_1 b(\omega_1, \omega_2) \frac{2\omega_2}{\omega_3} + 2\beta \frac{\omega_2}{\omega_3} W \bar{\delta}_2 \bar{d}_2, \quad (\text{A11})$$

and

$$r_{sps} = \sin \theta_2 b(\omega_2, \omega_1) \frac{2\omega_1}{\omega_3} - 2\beta \frac{\omega_1}{\omega_3} W \bar{\delta}_1 \bar{d}_1. \quad (\text{A12})$$

We notice that for *ssp* there is no surface contribution since $\chi_{z\parallel\parallel}^s = 0$. The different terms in above expressions are

$$\gamma = \frac{\epsilon_3(\omega_1 s_1 + \omega_2 s_2) / \omega_3 - \epsilon' s_3}{\epsilon_3 - \epsilon'}, \quad (\text{A13})$$

$$\beta = \frac{(\omega_1 s_1 + \omega_2 s_2) / \omega_3 - s_3}{\epsilon_3 - \epsilon'}, \quad (\text{A14})$$

$$\epsilon' = \frac{(\omega_1 \sin \theta_1 + \omega_2 \sin \theta_2)^2 + (\omega_1 s_1 + \omega_2 s_2)^2}{\omega_3^2}, \quad (\text{A15})$$

$$s_i = \sqrt{\epsilon_i - \sin^2 \theta_i}, \quad (\text{A16})$$

$$V = s_1 s_2 + \sin \theta_1 \sin \theta_2, \quad (\text{A17})$$

$$W = s_1 \sin \theta_2 - s_2 \sin \theta_1, \quad (\text{A18})$$

and finally the Fresnel factors are

$$F_p(\omega_i) = \frac{2 \cos \theta_i}{\epsilon_i \cos \theta_i + s_i}, \quad (\text{A19})$$

for p polarization, and

$$F_s(\omega_i) = \frac{2 \cos \theta_i}{\cos \theta_i + s_i}, \quad (\text{A20})$$

for s polarization.

- ¹X. D. Zhu, H. Suhr, and Y. R. Shen, *Phys. Rev. B* **35**, 3047 (1987); P. Guyot-Sionnest, J. H. Hunt, and Y. R. Shen, *Phys. Rev. Lett.* **59**, 1597 (1987).
- ²A. L. Harris, C. E. D. Chidsey, N. Y. Levinos, and D. N. Loiacono, *Chem. Phys. Lett.* **141**, 350 (1987).
- ³A. L. Harris, L. Rothberg, L. H. Dubois, N. J. Levinos, and L. Dhar, *Phys. Rev. Lett.* **64**, 2086 (1990).
- ⁴P. Guyot-Sionnest, P. Dumas, Y. J. Chabal, and G. S. Higashi, *Phys. Rev. Lett.* **64**, 2156 (1990).
- ⁵Q. Du, R. Superfine, E. Freysz, and Y. R. Shen, *Phys. Rev. Lett.* **70**, 2313 (1993).
- ⁶A. Peremans and A. Tadjedine, *Chem. Phys. Lett.* **220**, 481 (1994).
- ⁷A. Peremans and A. Tadjedine, *Phys. Rev. Lett.* **73**, 3010 (1994).
- ⁸M. S. Yeganeh, S. M. Dougal, R. S. Polizzotti, and P. Rabinowitz, *Phys. Rev. Lett.* **74**, 1811 (1995).
- ⁹P. Cremer, C. Stanner, J. W. Niemantsverdriet, Y. R. Shen, and G. Somorjai, *Surf. Sci.* **328**, 111 (1995).
- ¹⁰K. A. Friedrich, W. Daum, C. Klunker, D. Knabben, U. Stimming, and H. Ibach, *Surf. Sci.* **335**, 315 (1995).
- ¹¹A. Tadjedine, A. Peremans, and P. Guyot-Sionnest, *Surf. Sci.* **335**, 210 (1995).
- ¹²A. Le Rille, A. Tadjedine, W. Q. Zheng, and A. Peremans (unpublished).
- ¹³W. Daum, H.-J. Krause, U. Reichel, and H. Ibach, *Phys. Scr.* **T49**, 513 (1993).
- ¹⁴A. V. Petukhov, *Phys. Rev. B* **52**, 16 901 (1995).
- ¹⁵A. V. Petukhov and T. Rasing, *Surf. Sci.* **377-379**, 414 (1997).
- ¹⁶Bernardo S. Mendoza and W. Luis Mochán, *Phys. Rev. B* **53**, 4999 (1996).
- ¹⁷J. Sipe and G. I. Stegman, in *Surface Polaritons*, edited by V. M. Agranovich and D. L. Mills (North-Holland, Amsterdam, 1982).
- ¹⁸J. Rudnick and E. A. Stern, *Phys. Rev. B* **4**, 4274 (1971).
- ¹⁹B. S. Mendoza and W. L. Schaich, *Bull. Am. Phys. Soc.* **36**, 864 (1991).
- ²⁰J. A. Maytorena, W. Luis Mochán, and Bernardo S. Mendoza, *Phys. Rev. B* **51**, 2556 (1995); A. Chizmeshya and E. Zaremba, *ibid.* **37**, 2805 (1988); A. Liebsch and W. L. Schaich, *ibid.* **40**, 5401 (1989); A. Kiejna, *Surf. Sci.* **331-333**, 1167 (1995).
- ²¹W. Luis Mochán, Ronald Fuchs, and Rubén G. Barrera, *Phys. Rev. B* **27**, 771 (1983).
- ²²V. Mizrahi and J. E. Sipe, *J. Opt. Soc. Am. B* **5**, 660 (1988).
- ²³I. G. Currie, *Fundamental Mechanics of Fluids* (McGraw-Hill, New York, 1974).
- ²⁴P. Guyot-Sionnest and Y. R. Shen, *Phys. Rev. B* **38**, 7985 (1988).
- ²⁵P. S. Pershan, *Phys. Rev.* **130**, 919 (1963).
- ²⁶W. L. Schaich and B. S. Mendoza, *Phys. Rev. B* **45**, 14 279 (1992).
- ²⁷Robert C. Miller, *Appl. Phys. Lett.* **5**, 17 (1964).
- ²⁸M. I. Bell, *Phys. Rev. B* **6**, 516 (1972).
- ²⁹S. Scandolo and F. Bassani, *Phys. Rev. B* **51**, 6928 (1995).
- ³⁰J. D. Jackson, *Classical Electrodynamics*, 2nd ed. (Wiley, New York, 1975).
- ³¹Actually, we define the macroscopic polarization so that the induced current
- $$\vec{J} = \frac{\partial}{\partial t} (n\vec{p} - \frac{1}{2} \nabla \cdot n\vec{Q} + \dots) + c \nabla \times n\vec{\mu},$$
- is given by $\vec{J} = \partial \vec{P} / \partial t$. Therefore, $\vec{P} = (i/\omega_3) \vec{J}$ and we obtain Eq. (36).
- ³²D. E. Aspnes and A. A. Studna, *Phys. Rev. B* **27**, 985 (1983); R. F. Potter in *Handbook of Optical Constants of Solids*, edited by Edward D. Palik (Academic, New York, 1985) p. 465; D. F. Edwards, *ibid.*, p. 547.
- ³³W. Daum *et al.*, *Phys. Rev. Lett.* **71**, 1234 (1993).
- ³⁴J. F. McGilp *et al.*, *Opt. Eng. (Bellingham)* **33**, 3895 (1994).
- ³⁵C. Meyer *et al.*, *Phys. Rev. Lett.* **74**, 3001 (1995).
- ³⁶J. I. Dadap, *et al.*, *Phys. Rev. B* **53**, R7607 (1996).
- ³⁷P. Godefroy *et al.*, *Appl. Phys. Lett.* **68**, 1981 (1996).
- ³⁸L. E. Urbach, K. L. Percival, J. M. Hicks, E. W. Plummer, and H. L. Dai, *Phys. Rev. B* **45**, 3769 (1992).
- ³⁹G. Lüpke, D. J. Bottomley, and H. M. van Driel, in *Proceedings IEEE Nonlinear Optics '94*, IEEE Cat. #94CH3370-4 (IEEE, Piscataway, NJ, 1994), p. 151; *Phys. Rev. B* **49**, 17 303 (1994); J. Bloch, G. Lüpke, S. Janz, and H. M. van Driel, *ibid.* **45**, 12011 (1992).
- ⁴⁰P. Guyot-Sionnest, A. Tadjedine, and A. Liebsch, *Phys. Rev. Lett.* **64**, 1678 (1990).
- ⁴¹W. L. Mochán and Bernardo S. Mendoza, *J. Phys.: Condens. Matter* **5**, A183 (1993).
- ⁴²B. S. Mendoza, *J. Phys.: Condens. Matter* **33A**, A181 (1993).
- ⁴³Bernardo S. Mendoza and W. Luis Mochán, *Phys. Rev. B* **53**, R10 473 (1996).
- ⁴⁴Bernardo S. Mendoza and W. Luis Mochán, *Phys. Rev. B* **55**, 2489 (1997).